NANO LETTERS

pubs.acs.org/NanoLett

Optical Manipulation with Planar Silicon Microring Resonators

Shiyun Lin, Ethan Schonbrun, and Kenneth Crozier*

School of Engineering and Applied Sciences, Harvard University, Cambridge, Massachusetts 02138

ABSTRACT We demonstrate optically trapping of microparticles on silicon microring resonators. Once trapped on a microring, a particle can be confined in an optical potential with a depth of 25 k_BT over the entire microring's circumference. The particles are propelled around the microring at hundreds of micrometers per second, producing periodic revolutions at a few hertz. We anticipate that the increased force and highly accurate positioning obtainable with this system will lead to various nanomanipulation applications.

KEYWORDS Optical trapping, microring, resonator, nanomanipulation

Optical trapping enables noncontact manipulation of micro and nanoparticles with extremely high precision.[1] Traditionally, optical forces have been exerted on particles in solution using laser beams focused by high numerical apertures (NA) lenses.[2] In addition to localizing a particle to a single spot, high NA lenses can project other patterns such as lines,[3] rings,[4,5] or periodic interference patterns[6,7] to exert optical forces on beads over larger areas. A major limitation of this technique however, is that when a laser beam is spread over a larger area, the optical force is reduced in proportion to the decreased intensity.

Alternatively, the evanescent fields around planar photonic devices enable strong optical gradient and scattering forces to be exerted on particles in the near field produced by integrated photonic structures.[8,9] Planar waveguides[10,11] are capable of localizing particles near their surface and propelling them in the propagation direction of the guided wave. Integrated photonic resonators, based on photonic crystals,[12,13] surface plasmon structures,[14,15] and silica microspheres,[16] have also been used to exert optical forces on particles in suspension. Compared to a waveguide trapping configuration, resonant cavity trapping presents two primary advantages: (1) the high field confinement in a cavity leads to strong optical force enhancement, and (2) cavity perturbation induced by the trapped object could serve as a highly sensitive probe for analyzing the physical properties (size, refractive index, absorption) of the objects.[17,18] Unlike free space optical trapping geometries, optical waves propagating through waveguide devices stay highly confined over larger distances, and consequently are capable of delivering larger optical forces over larger areas. Trapping on planar ring resonators has also been reported recently,[19] however, careful analysis of the force enhancement, trapping stiffness, and potential depth has not been addressed yet.

Here, we demonstrate an on-chip optical trapping system using planar microring resonators with radii of 5 and 10 μm. Figure 1a shows the schematic diagram of our planar microring cavity trapping system. We observe trapping of 1.1 μm diameter polystyrene particles that revolve around the microring at a few hertz and are stable for several minutes. Depending on the particle concentration and flow conditions, single or multiple particles can be simultaneously trapped. Supporting Information Movie 1 shows three particles being delivered along the bus waveguide to a 5 μm microring, where they are then trapped at a power of 5 mW. A trapped particle moves around the microring with approximately constant velocity that is dependent on the power coupled into the bus waveguide and the finesse of the microring resonator. In this Letter, we experimentally mea-

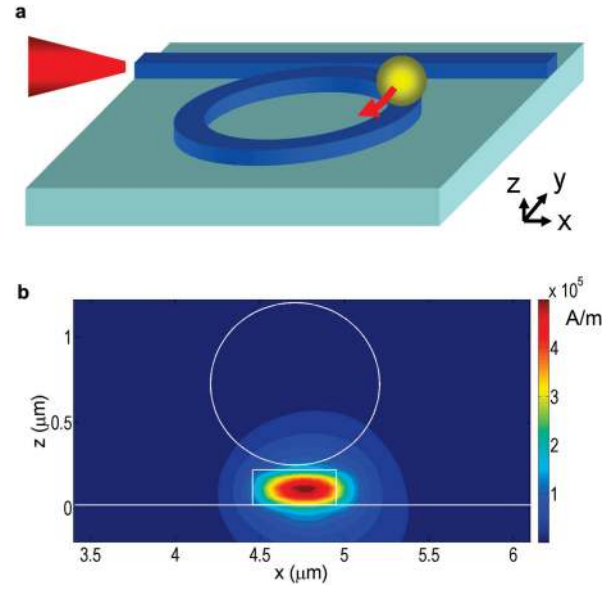

FIGURE 1. Microring trapping system. (a) Schematic diagram of planar microring cavity trapping system; (b) cross section of the instantaneous field distribution (Hx: x-component of magnetic field) of the whispering-gallery mode of the microring by 3D-FDTD simulation with a 1 W input power in the waveguide. The outer edge of the microring is at $x \approx 5$ μm.

* To whom correspondence should be addressed. E-mail: kcrozier@seas.harvard.edu.

Received for review: 2/10/2010
Published on Web: 06/14/2010

DOI: 10.1021/nl100501d | *Nano Lett.* **2010,** *10,* 2408–2411

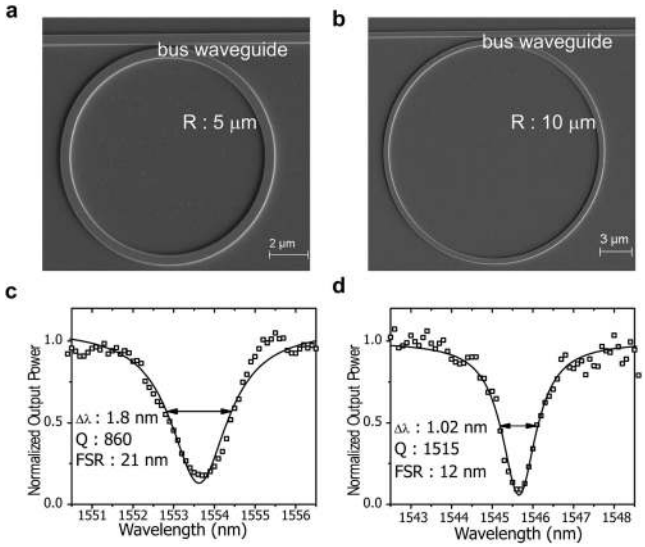

FIGURE 2. SEM images and transmission spectra of microring resonators. (a,b) SEM image of microring with radii of (a) 5 μm and (b) 10 μm. (c,d) Transmission spectra of rings with radii of (c) 5 and (d) 10 μm, respectively. Black squares are measured output powers. Lines are the Lorentzian fits to the measured data. The quality factor (Q) of the 10 μm microring is 1515, which is larger than that of the 5 μm microring (Q = 860) due to a smaller bending loss. Free spectral range (FSR) and the full width of the half-maximum of the resonance peak ($\Delta\lambda$) are also shown in (c,d).

sure the particle velocity as a function of coupling power and compare to numerical simulations. In addition, we measure the shape and depth of the two-dimensional optical potential over the ring by tracking a particle's position over several revolutions with a high speed camera.

Microrings with radii of 5 and 10 μm and widths of 500 nm are fabricated on an SOI wafer with a 220 nm top Si layer using electron beam lithography and reactive ion etching. Light is coupled into and out of the resonator from a bus waveguide with the same width and a ring-bus gap of 150 nm. The output of a tunable laser (HP8168, near λ = 1550 nm) is amplified by a high power C-band erbium-doped fiber amplifier (EDFA) and launched into the waveguide to excite TM modes. A typical field distribution (Hx: x-component of magnetic field) on a $x-z$ plane cross section is shown in Figure 1b. A lens-tipped fiber with a focal spot size of 3 μm is used to couple light into the waveguide and results in a coupling loss of approximately 10 dB. A PDMS microfluidic channel with a height of 50 μm and a width of 200 μm is bonded on top of the resonator structure. Fluorescent polystyrene particles with diameters of 500 nm are injected into the channel during the trapping tests. A green laser (λ = 532 nm, P = 0.75 mW) is used to excite the fluorescent emission, which is imaged by a microscope objective onto a CCD camera.

The transmission spectra of microrings with radii of 5 and 10 μm are shown in Figure 2. Field intensity enhancement factor G in microring cavities can be expressed as $G = F/2\pi^*(1 - T)$, where F is the finesse, and T is the transmission coefficient at the resonance frequency[20] Finesse is calculated by F = FSR/$\Delta\lambda$, where FSR is the free spectral range, and $\Delta\lambda$ is the full width of the half-maximum of the resonance peak. The measured values for Q and FSR for both microrings are also shown in the inset of Figure 2c,d. A field intensity enhancement of 1.76 for the 10 μm microring is achieved, compared to a 1.50 intensity enhancement for the 5 μm microring. The field enhancement leads to larger optical forces with the microrings than with straight waveguides.

In Figure 3, the measured and simulated power dependence of the optical force along the light propagation direction is shown for a straight waveguide and the 5 μm radius microring resonator. The measured longitudinal force in the Figure 3 is calculated by the Stokes' drag formula, $F = 6\pi r\eta v$ where r is the particle radius and v is the measured particle velocity. We assume no significant temperature change during the measurement, and the room temperature dynamic viscosity of water ($\eta = 8.9 \times 10^{-4}$ Pa·s) is used in the calculation. The simulated force is calculated using a Maxwell stress tensor formalism based on 3D-FDTD simulation. The Debye length of our particle solution is 21 ± 9 nm. In ref 15, the authors found that the gap in their near-field optical trapping experiments was slightly larger than the Debye length. While we do not know the precise gap between the particle and the waveguide surface, for the calculation we assume a gap of 30 nm. Both measured curves show a linear increase of optical force as a function of guided power and are close to the values predicted by simulations. Possible sources of error include temperature variations, transient flow velocities, and increased drag due to proximity of the silicon-water interface. The minimum required guided power for stable trapping on the waveguide is 4.7 mW, which is comparable to other reported results of trapping on waveguides.[5,6] However, particles can be trapped and propelled along the microring resonator with a guided power as low as 0.67 mW. At the same guided power level, the measured velocity of particles on a microring is 5−8 times larger than that on a waveguide.

Because of the resonant response of the microring, the optical force also depends on the incident wavelength. Figure 3b shows the average velocity as a function of excitation wavelength of eight trapped beads that are simultaneously circulating the 5 μm microring. In this measurement, a guided power of 3 mW in the bus waveguide is used. The number of trapped particles is fixed (8 particles) through the use of a flow with a relatively low particle concentration during the measurement. For reference, the spectrum of an unloaded ring is also plotted (black squares). The velocity of the eight particles strongly peaks at a wavelength that is red shifted by 1 nm compared to the unloaded microring. This red shift of resonance is due to optical perturbation resulting from the trapped polystyrene beads.

In addition to a large longitudinal force along the circumference of the ring, the particle also experiences a large transverse force across the radial direction. This force keeps the particle stably trapped, enabling the particle to circulate

DOI: 10.1021/nl100501d | Nano Lett. 2010, 10, 2408--2411

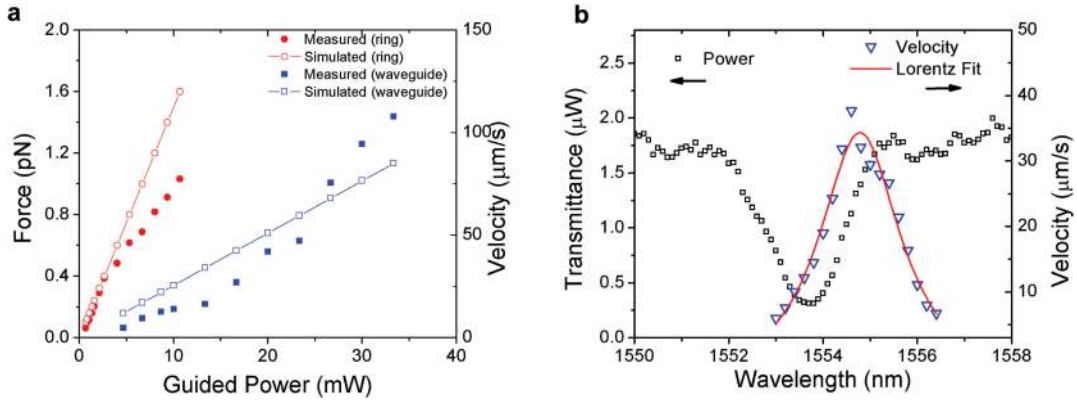

FIGURE 3. Longitudinal optical force. (a) Measured velocity (right axis) and optical force (left axis) on circling particles plotted as a function of input power for straight waveguide and microring ($r = 5\ \mu$m) trapping. The squares and circles correspond to measured data on resonators, and straight waveguides, respectively, and lines with open symbols correspond to simulation results. (b) Transmission spectrum of the microring resonator near a TM resonance mode, and the circling velocity of polystyrene beads, as a function of wavelength. The blue triangles are experimentally measured data and the red trace is a Lorentzian fit.

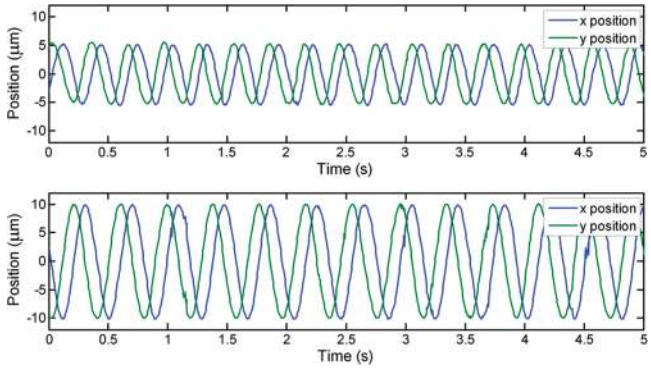

FIGURE 4. Tracked positions of a single particle trapped on the microring. (a) Particle trapped on a 5 μm microring. (b) Particle trapped in a 10 μm microring.

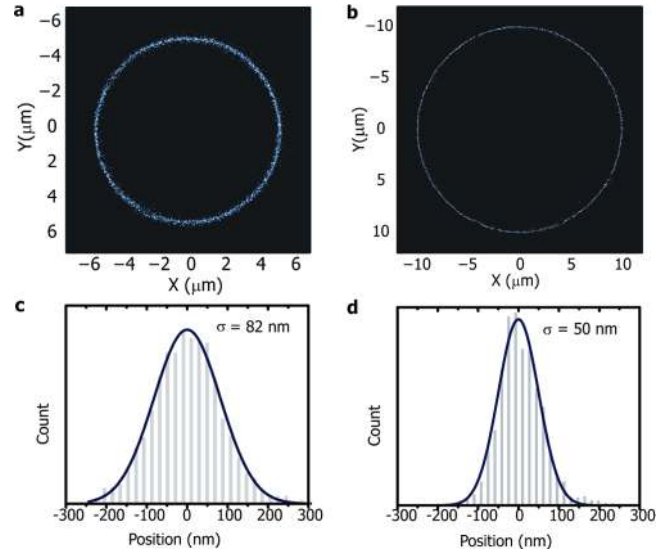

FIGURE 5. Two dimensional histograms of trapped particle positions. (a,b) Two-dimensional histograms of a trapped particle over the (a) 5 and (b) 10 μm microring. (c,d) One-dimensional histograms along the radius axis for the (c) 5 μm and (d) 10 μm microring. Light is coupled to the ring from a bus waveguide above the ring, where the guided mode travels from right to left. Data is plotted as a function of r, the radial direction.

for several minutes, limited only by the flow conditions in the microfluidic channel. Supporting Information Movie 2 shows two particles are trapped on the 10 μm ring. Figure 4 shows the x and y positions of a particle trapped on the 5 and 10 μm microring resonators. This is measured by calculating the centroid of the trapped particle from a video taken at 200 frames per second. The powers coupled into the bus waveguide are 9 and 4.5 mW for 5 and 10 μm rings, respectively. As can be seen in Figure 4, the trajectories of the bead are periodic with frequencies of 3.4 and 2.5 Hz for the 5 and 10 μm microring, respectively, corresponding to velocities of 110 ± 10 and $160 \pm 5\ \mu$m/s. Bend loss reduces the field enhancement in the microring at regions further away from the bus waveguide, resulting in a slower bead velocity in these regions.

By observing the particle position through several revolutions, the trapping potential can be mapped out. Figure 5 shows plots of two-dimensional histograms of particle position for the 5 and 10 μm microring for the same illumination power as shown in Figure 4. The histograms comprise 15 s of data, corresponding to approximately 51 and 38 revolutions, respectively. The bus waveguide runs along the top of the ring, where the guided mode propagates from right to left. Using the equipartition theorem, the radial trap stiffness can be calculated from the measured thermal motion shown in the histograms.[21] The radial trap stiffness is found by calculating the standard deviation σ of the difference between the particle position and the center of microring through out the entire circumference of the microring. The measured σ are 82 and 50 nm for the 5 and the 10 μm microring, respectively. From these particle distributions, the radial trap stiffnesses are found to be 0.62 pN/μm for the 5 μm ring and 1.66 pN/μm for the 10 μm ring. As can also be seen in Figure 5a,b, the 10 μm microring localizes the particle more stiffly than the 5 μm microring.

DOI: 10.1021/nl100501d | Nano Lett. 2010, 10, 2408--2411

In addition to the slightly larger finesse and field enhancement, the increase in relative force of the 10 μm microring is likely also due to better coupling efficiency in this device. Both rings, however, stiffly confine the trapped particle over their entire circumferences, which have lengths of 31 and 62 μm. From simulations, we find that the maximum force exerted on a trapped particle on a microring occurs when the bead is approximately $w/2$ away from the trap center, where w is the width the waveguide. At $w/2$ from the trap center, the product of trap stiffness with extension $k \times w/2$ is 0.16 pN for the 5 μm microring at a power of 9 mW, corresponding to a potential depth of 9.3 k_BT. Similarly, a potential depth of 25 k_BT is achieved for the 10 μm microring at a power of 4.5 mW. Here, the potential depth is calculated by $U = k \times (w/2)^2$, assuming a Gaussian potential well. This expression gives the potential depth of a Gaussian potential well, where k is the trap stiffness at the center and $w/2$ is the position at which the gradient maximum force occurs. This is a reasonable assumption as the potential associated with gradient force and the intensity are proportional in the dipolar limit. The 3D FDTD simulations confirm that the intensity on the top of the ring follows a Gaussian distribution.

In summary, we have experimentally demonstrated optical trapping of dielectric particles on Si microring resonators. The particles are stably propelled around the ring circumference with velocities as high as 180 μm/s for several minutes. We measure a 5−8 times enhancement of the optical force for a microring of radius of 5 μm, compared to a straight waveguide. In addition, the power required for stable trapping is reduced to be as low as 0.67 mW. A 25 k_BT potential depth is measured from a particle position histogram for the 10 μm microring. We expect to realize all-optical on-chip manipulation (routing, delivery, and storage) of nanoparticles and biomolecules using this resonator platform.

Acknowledgment. The authors would like to thank J. Hu for fruitful discussions. This work was supported by the Harvard Nanoscale Science and Engineering Center (NSEC), which is supported by the National Science Foundation (NSF). Fabrication work was carried out in the Harvard Center for Nanoscale Systems (CNS), which is also supported by the NSF.

Supporting Information Available. Movies recorded by a CCD camera at 60 frames per second are provided. Movie 1 illustrates three particles being delivered along the bus waveguide to a 5 mm microring and trapped on the 5 mm ring. Movie 2 shows two particles are steadily trapped on the 10 mm ring. This material is available free of charge via the Internet at http://pubs.acs.org.

REFERENCES AND NOTES

(1) Grier, D. G. *Nature* **2006**, *424*, 21–27.
(2) Ashkin, A. *Proc. Natl. Acad. Sci. U.S.A.* **1997**, *94*, 4853–4860.
(3) Biancaniello, P. L.; Crocker, J. C. *Rev. Sci. Instrum.* **2006**, *77*, 113702.
(4) Curtis, J. E.; Grier, D. G. *Phys. Rev. Lett.* **2003**, *90*, 133901.
(5) Garces-Chaves, V.; McGloin, D.; Padgett, M. J.; Dultz, W.; Schmitzer, H.; Dholakia, K. *Phys. Rev. Lett.* **2003**, *91*, No. 093602.
(6) MacDonald, M. P.; Spalding, G. C.; Dholakia, K. *Nature* **2003**, *426*, 421–424.
(7) Schonbrun, E.; Piestun, R.; Jordan, P.; Cooper, J.; Wulff, K.; Courtial, J.; Padgett, M. J. *Opt. Express* **2005**, *13*, 3777–3786.
(8) Kawata, S.; Tani, T. *Opt. Lett.* **1996**, *21*, 1768–1770.
(9) Yang, A. H. J.; Moore, S. D.; Schmidt, B. S.; Klug, M.; Lipson, M.; Erickson, D. *Nature* **2009**, *457*, 71–75.
(10) Gaugiran, S.; Geti, S.; Fedeli, J. M.; Colas, G.; Fuchs, A.; Chatelain, F.; Derouard, J. *Opt. Express* **2005**, *13*, 6956–6963.
(11) Schmidt, B. S.; Yang, A. H. J.; Erickson, D. Lipson. *Opt. Express* **2007**, *22*, 14322–14334.
(12) Lin, S.; Hu, J.; Kimerling, L.; Crozier, K. *Opt. Lett.* **2009**, *34*, 3451–3453.
(13) Mandal, M.; Serey, X.; Erickson, D. *Nano Lett.* **2010**, *10*, 99–104.
(14) Righini, M.; Zelenina, A. S.; Girard, C.; Quidant, R. *Nat. Phys.* **2007**, *3*, 477–480.
(15) Wang, K.; Schonbrun, E.; Crozier, K. B. *Nano Lett.* **2009**, *9*, 2623.
(16) Arnold, S.; Keng, D.; Shopova, S. I.; Holler, S.; Zurawsky, W.; Vollmer, F. *Opt. Express* **2009**, *17*, 6230–6238.
(17) Vollmer, F.; Arnold, S. *Nat. Methods* **2008**, *5*, 591–596.
(18) Zhu, J.; Ozdemir, S. K.; Yun-Feng, X.; Li, L.; Lina, H.; Chen, D.; Yang, L. *Nat. Photonics* **2010**, *4*, 46–49.
(19) Mandal, S.; Serey, X.; Erickson, D. *Nano Lett.* **2010**, *10* (1), 99–104.
(20) Saleh, B. E. A.; Teich, M. C. *Fundamentals of Photonics*; John Wiley & Sons, Inc.: New York, 1991.
(21) Neuman, K. C.; Block, S. M. *Rev. Sci. Instrum.* **2004**, *75*, 2787–2809.

DOI: 10.1021/nl100501d | *Nano Lett.* **2010,** *10,* 2408--2411